Stasis in the adaptive landscape of two ecologically similar and sympatric damselfly species

Anjali Gupta[1, 2†], Erik I. Svensson[2‡], Henrik Frietsch[2] and Masahito Tsuboi[2‡]

1. Department of Biological Sciences, Indian Institute of Science Education and Research Mohali, Sector 81, SAS Nagar, Mohali, Punjab 140306, India
2. Department of Biology, Lund University, Sölvegatan 37, 22362 Lund, Sweden

[†]Current address: Department of Ecology & Evolutionary Biology, University of Kansas, Lawrence, KS 66045, United States

[‡]Corresponding authors: Erik I. Svensson (erik.svensson@biol.lu.se), Masahito Tsuboi (masa.tsuboi@gmail.com)

Running title: Comparison of adaptive landscape in damselflies

Acknowledgements: We thank Stephen de Lisle and Viktor Nilsson-Örtman for discussions on earlier versions of analyses and manuscripts, Seth Donoughe for helping us with image processing, and Benjamin Jarrett, Emma Kärrnäs, Moritz Lürig, Ayushi Mahajan, Muskaan, Sofie Nilén, Karolina Pehrson, Moa Metz and Kajsa Svensson for assisting our field work. We also thank constructive comments from Gabrielle Marroig, Michel Morrissey, and David Punzalan for an earlier version of this manuscript. This study was supported by the Swedish Research Council grant for EIS (2020-03123) and MT (2016-06635).

Conflict of Interest: We have no conflicts of interest to declare.

Data accessibility: Data and code will be archived in DRYAD upon acceptance.

Abstract

Following the development of regression-based methods to estimate natural and sexual selection, evolutionary biologists have quantified the strength, mode and direction of selection in natural populations. Although this approach has been successful, its limitations include lack of replication across species, compromising the generality of the inferences beyond microevolutionary time scales. Here, we carried out a comparative selection study on wing shape and body size across multiple populations of two closely related and ecologically similar pond damselflies: *Enallagma cyathigerum* and *Ischnura elegans* (family Coenagrionidae). Our data revealed directional selection on body size in females and weak stabilizing selection on wing shape in both sexes, and these selection regimes were shared between the species. In contrast, sexual selection on male body size was curvilinear and divergent between species. By analyzing selection on the fine-grained spatial scale, we found that selection of male body size was shaped by the local social organization, and the relationship between socioecological indices and directional selection was consistent between the two species. Our study illustrates a case of stasis in the adaptive landscape caused by ecological similarity between taxa, supporting the idea that a shared ecological niche may result in a stable adaptive zone lasting millions of years.

Key words: Adaptive landscape, adaptive zone, natural selection, sexual selection, *Ischnura elegans*, *Enallagma cyathigerum*

Introduction

Since Russell Lande and Stevan Arnold introduced regression-based statistical methods to quantify natural and sexual selection four decades ago (Lande & Arnold, 1983), evolutionary biologists have sought to describe and understand the causes of phenotypic selection in nature (Endler, 1986; Mitchell-Olds & Shaw, 1987; Wade & Kalisz, 1990; Kingsolver & Diamond, 2011). This has resulted in a rich scientific literature about the strength, mode and direction of selection in wild populations of animals and plants (Kingsolver *et al.*, 2001; Siepielski *et al.*, 2009, 2011, 2013, 2017; Kingsolver & Diamond, 2011). However, several methodological and conceptual problems remain (Mitchell-Olds & Shaw, 1987; Wade & Kalisz, 1990; Hereford *et al.*, 2004; De Lisle & Svensson, 2017), including the lack of our understanding of whether and how estimates of phenotypic selection measured at contemporary populations are related to divergence across populations, species, or higher taxa (e.g. macroevolution). The adaptive landscape is a conceptual framework to unify phenotypic selection within populations with the pattern of macroevolution (Arnold *et al.*, 2001; Svensson & Calsbeek, 2012). Under this framework, populations are conceptualized as evolving on fitness surfaces, where they are subject to selection, genetic drift and mutation (Lande, 1976). Populations are expected to climb the closest adaptive peak in the direction where short-term fitness is maximized (Wright, 1932) whereas genetic correlations can bias the evolutionary trajectories towards directions with high amount of additive genetic variance (Schluter, 1996; Walsh & Blows, 2009). Estimates of selection coefficients and correlational selection (Phillips & Arnold, 1989; Brodie *et al.*, 1995; Svensson *et al.*, 2021) capture local landscape topography, which can in turn be used to infer the dynamics of landscape itself (Chevin & Lande, 2015; De Villemereuil *et al.*, 2020). Comparative studies of selection in different populations and/or between closely related species therefore link phenotypic selection at the microevolutionary level with macroevolutionary dynamics. However, such studies are still relatively few, mainly because of the logistical challenges to obtain sufficient spatial and temporal replication (Nishida, 1994; Gosden & Svensson, 2008; Siepielski *et al.*, 2009, 2017; Punzalan *et al.*, 2010; De Villemereuil *et al.*, 2020).

In a seminal paper, Arnold et al., 2001 envisioned that the integration of microevolution and macroevolution requires a shift from a static to a dynamic view of adaptive landscape. It triggered an important conceptual shift in the literature of phylogenetic comparative studies (Estes & Arnold, 2007; Uyeda *et al.*, 2011; Hansen, 2014), where the parameters of an Ornstein-Uhlenbeck model began to be recognized as descriptors of the dynamics of adaptive zone–a collection of adaptive landscapes inhabited by populations and species that share ecological mode of life (Simpson, 1944; Hansen *et al.*, 2008) rather than the dynamics of species evolving on a fixed adaptive zone. Thus, the adaptive landscape estimated from present-day populations and the adaptive zone estimated from a dataset that contains multiple species can be conceptually related to study the link between contemporary selection and macroevolutionary dynamics. However, this idea is currently considered a metaphor with limited bearings on empirical research, because many previous studies have shown that phenotypic selection often fluctuates over short time scales (Kinnison & Hendry, 2001; Grant & Grant, 2002; Gosden & Svensson, 2008; Siepielski *et al.*, 2017) and that stabilizing selection is not necessarily a common form of selection in nature (Kingsolver & Diamond, 2011). Such findings are at odds with the core premise of the adaptive zones–the assumption that adaptive phenotypes are stable over hundreds of millions of years. Therefore, to construct an operational research program of the adaptive landscape "*as a conceptual bridge between micro- and macroevolution*" (Arnold *et al.*, 2001), we need to elucidate how dynamic adaptive landscapes are

at the population level, and if this does or does not result in a stable adaptive zone at macroevolutionary time scale.

The stability of ecological niche has long been a major hypothesis to explain the persistence of adaptive zone. In the classic work on the evolution of high-crown cheek teeth (hypsodonty) in horses, Simpson, 1944 argued that the evolution of hypsodonty in the early to middle Miocene reflects the spread of savanna and grassland habitats during this era. A microevolutionary analogue to this argument is abound in the literature of phenotypic selection. For example, it has been suggested that trait-fitness covariances (i.e. selection gradients) are not necessarily causal and should be viewed as preliminary hypotheses in need of experimental verification through trait manipulations (Mitchell-Olds & Shaw, 1987). Furthermore, it has also been argued that functional analysis of selective agents or detailed field observations in natural settings are necessary to identify environmental agents, demographic factors and ecological causes behind observed selection (Svensson & Sinervo, 2000; MacColl, 2011; Opedal, 2021). All this work emphasize ecology as a key variable explaining variation in phenotypic selection and local adaptive landscapes. Thus, ecology can provide key insights to bridge micro- and macroevolution, but relatively few studies have identified the ecological causes behind phenotypic selection in natural populations (Arnqvist, 1992; Grant & Grant, 2002; Gosden & Svensson, 2008; Punzalan *et al.*, 2010).

The insect order Odonata (damselflies and dragonflies) is a popular system for studies of phenotypic selection because a rich background knowledge of natural history (Corbet, 1999) enables characterization of the adaptive landscape in different environmental and ecological contexts. Here, we study two ecologically and phenotypically similar sympatric damselfly species: the common bluetail damselfly (*Ischnura elegans*) and the common bluet (*Enallagma cyathigerum*). These two species and other members of the family Coenagrionidae (pond damselflies) have similar ecological niches, show evidence of neutral community dynamics and may therefore fluctuate in abundances due to ecological drift (McPeek & Brown, 2000; Siepielski *et al.*, 2010). Molecular phylogenetic evidence suggest that these two genera have been separated by >12 million years (Swaegers *et al.*, 2014; Callahan & McPeek, 2016; Blow *et al.*, 2021). The high ecological similarity of these two closely related species from two different genera provide a unique opportunity to investigate if the adaptive zone has remained stable for millions of years, while simultaneously considering the local adaptive landscapes that vary on fine-grained spatial and temporal scales. Previous selection studies suggest that spatial variation in phenotypic selection in *I. elegans* is partly governed by female color polymorphism dynamics (Gosden and Svensson 2008) and these female colour morphs experience negative frequency-dependent selection (Svensson *et al.*, 2005; Le Rouzic *et al.*, 2015). We hypothesize that spatially and temporally fluctuating short-term selection in these damselflies may result in stable adaptive zones over longer macroevolutionary time scales.

We have three objectives in this study. First, we estimated univariate and multivariate selection on two important fitness-related traits – body size and wing shape, and compared these within and between species. Second, we quantified demographic and mating system parameters across multiple populations of these two species. These demographic and mating system parameters include the opportunity for sexual selection (Arnold & Wade, 1984), mating frequencies, male and female densities, operational sex ratio (OSR) and the frequency of male-mimicking female color

morphs ("androchrome females"). These mating system parameters provide information about the local sexual selection regimes, male-male competition (opportunity for sexual selection, OSR, male density) and the intensity of male mating harassment and sexual conflict (mating frequencies and the frequency of androchrome female morphs see (Svensson *et al.*, 2005; Gosden & Svensson, 2009; Takahashi *et al.*, 2014; Blow *et al.*, 2021). Finally, by combining information from these different sources about the ecological and social causes of selection, we aim to understand and explain the stability and dynamics of the adaptive zones in these pond damselflies.

Materials & Methods

Study system: We studied two species of damselflies, the common bluet, *Enallagma cyathigerum* and the common bluetail damselfly, *Ischnura elegans* in the family Coenagrionidae (Odonata; Zygoptera). These species are generalist predators that feed on small flying insects and they occur in diverse aquatic habitats, typically open landscapes in ponds, lake shores, and slow flowing streams (Smallshire & Swash, 2020). Females of both species are polymorphic; females of *E. cyathigerum* exhibit two color morphs: androchrome (mature females with blue thorax mimicking males; Fig. 1A *ii*) and gynochrome (mature females with olive-green thorax; Fig. 1A *iii*), while females of *I. elegans* exhibit three color morphs during the adult stage: androchrome (mature females with blue thorax; Fig. 1A *v*), infuscans (Fig. 1A *vi*) and infuscans-obsoleta (Fig. 1A *vii*, (Svensson *et al.*, 2020; Willink *et al.*, 2020). Mating system of both species are characterized by scrambling competition, where males are non-territorial and found resting or flying near the waterbody, chase females that approach the waterbody, and compete for the opportunity for mating. A male that successfully clasps a female will form the "tandem position", followed by the formation of "a mating wheel" (Fig. 1D) during which egg fertilization takes place (Corbet, 1999).

Field work: Field surveys were carried out to collect *I. elegans*, and *E. cyathigerum* at 20 different field sites in and around Lund, Sweden. Field sampling was conducted at small ponds in the following localities: Borgeby, Bunkeflostrand, Flackarp, Flyinge 30 A1, Flyinge 30 A3, Genarp, Gunnesbo, Hoje A14, Hoje A6, Hoje A7, Habo Gard, IKEA, Ilstorp, Krutladan, Ladugårdsmarken, Lomma, Lunnarp, Råbydammen, Vombs vattenverk, and Vombs Bruksgård (Fig. S1). Individuals were captured using hand-held nets while slowly walking around waterbodies. Upon capture of individuals flying without a partner, we examined sex and kept males and females separately in small net cages. Individuals found as either a tandem or as a copulating couple were kept in plastic cups. We visited these populations between the hour of 08.00 and 13.00 in all partially or fully sunny days with temperature >15°C in May, June and July of 2020 and 2021. At each visit, we sampled between 20 and 30 minutes, and between 3-5 people participated in the sampling. The captured damselflies were kept in cooling bags to protect them from overheating, and were brought back to the lab for recording phenotypic data and setting up mated females for egg-laying for fecundity measurements. For each individual, we recorded sex, female morph, and morphometric measurements (see subsequent section for more detail). The dataset obtained from this field survey include 58 sampling visits to capture *I. elegans* (in 2020 and 2021) and 27 sampling visits to capture *E. cyathigerum* (in 2021), and constitutes in total of 497 single males, 236 single females, and 524 couples of *I. elegans* and 420 single males, 181 single females, and 411 couples of *E. cyathigerum*. This dataset was used to estimate selection gradients presented further in this study.

In a complementary field study, we quantified social organization and mating systems of *I. elegans* and *E. cyathigerum*. This was part of a community survey where we captured individuals of damselflies and dragonflies regardless of the species identity along predefined transects, with the aim of quantifying species composition, operational sex-ratio and density of local Odonata fauna. At each visit, 3-5 people sampled between 10-20 minutes, who identified and recorded all captured individuals in terms of species, sex, female color morph, sexual maturity and mating status (either captured as single or copula/tandem). After recording this information, animals were released. We used data of *I. elegans* and *E. cyathigerum* from four seasons (2018-2021) that were collected during a total of 366 visits. These data constitute a total observation of 3527 single males, 1788 single females, and 630 couples of *I. elegans* and 3031 single males, 403 single females, and 282 couples of *E. cyathigerum*. This dataset was used to compare and quantify differences in mating system and social organizations between these two species.

Fitness components: We measured two fitness components: (1) mating success that characterizes sexual selection in males and (2) fecundity that characterizes natural selection in females. Sexual selection on males was estimated by comparing the phenotypes of mated males with unmated males upon capture in the field. Males that were captured in tandem or in a copula were classified as 'mated' and assigned a mating success of '1', while males that were captured solitary were classified as 'single' and their mating success were assigned to '0'. This is an established technique of quantifying mating success in damselflies (Gosden & Svensson, 2008; Steele *et al.*, 2011). To measure female fecundity, we placed females captured in mated couples in small plastic cups with moist coffee filter to let the female lay eggs for 48hrs. The number of eggs laid by each female was subsequently counted. The number of eggs laid during this time interval likely reflects the recent ecological conditions a given female has experienced preceding oviposition, and should capture her past history of food intake rates and ambient temperatures (Svensson & Abbott, 2005; Svensson *et al.*, 2020). This fecundity measure thus provides a measure of fitness and natural selection in females. Although our cross-sectional measure of fitness is often considered noisy compared to longitudinal measures such as lifetime reproductive success, this limitation is less severe in short-lived insects (Nishida, 1989) such as pond damselflies which typically live for only a few days as reproducing adults (Corbet, 1999).

Morphometric measurements and wing image acquisition: We obtained digital images of all captured individuals using a scanner (CanoScan 5600F) at a resolution of 600 dpi to measure body size. Five linear measurements were taken for each individual to capture different aspects of the body size: total body length, thorax width, abdomen length, wing length, and width of the S4 segment (Fig. 1B). Individuals were measured from these photographs using the computer program, Fiji (Schindelin *et al.*, 2012). All measurements were originally recorded in units of pixel, which was then converted to millimeter (mm) based on a conversion between mm and pixel. After the scan has been completed, individuals were sacrificed by exposing them to cold temperature. From sacrificed individuals, we dissected fore- and hindwings from both left and right side of the body. Dissected wings were then placed in a wet coffee filter, covered with a transparent plastic sheet, then scanned at a resolution of 2000 dpi. We obtained images for a total of 5764 wings belonging to *E. cyathigerum*, and a total of 7704 wings belonging to *I. elegans*.

Automated assay of wing shape using ML-morph: We used a recently developed machine learning tool "ML-morph" (Porto & Voje, 2020) to measure the x-y coordinates of 17 landmark that characterize wing venation patterns (Fig. 1C). First, a training set was constructed to train ML-morph to identify the landmark positions in the wing image. We used a training set containing 400 wing images that was landmarked manually using Imglab version 1.18 (compiled from Python module dlib-19.23). These 400 images subset in the training set contained a random mixture of 100 images of the 4 wings (right forewing, right hindwing, left forewing, left hindwing) of a male *I. elegans*, 100 images of a female *I. elegans*, 100 images of a male *E. cyathigerum*, and 100 images of a female *E. cyathigerum*. This training set represents variation in wing shape with respect to sex, species, and fore- or hind-wing assignment, that are considered as main source of variation in our sample set.

We used *shape.predictor* function of the ML-Morph to train the algorithm for landmarking the wing. Then, we tested the ability of ML-Morph to landmark wings accurately using *shape.tester* function, where we compared automated landmarking by ML-morph to manual landmarks, which responded to 99.2% precision in the landmarking using automation in a test set build from the training set. Finally, we applied *shape.predictor* function to landmark the remaining image set that have not been landmarked. All landmarked images were later checked manually for any errors, and inconsistent landmarks across all images were corrected. We removed 357 images (178 for *I. elegans* and 179 for *E. cyathigerum*) from the dataset before analysis because they contained an injured/broken wing where position of 1 or more landmarks could not be deduced accurately. Examination of erroneous images were done by one observer (AG).

Geometric morphometrics and dimension reduction: The wing data obtained from ml-Morph were standardized through geometrics morphometrics analysis. We performed a Generalized Procrustes Analysis (GPA) on the 17 landmarks including all measured wings using geomorph package version 4.0.5. GPA transforms the landmarks by rotating, aligning, and scaling so that the resulting landmarks (i.e., aligned coordinates) describe the wing shape alone. The aligned coordinates, however, still have 30 dimensions, and dimensional reduction was necessary for further analyses. We employed two complementary approaches for dimension reduction. First, we performed a principal component analysis (PCA) on the covariance matrix containing the aligned coordinates of both species to reduce dimensionality of the major axis of morphological variation. Second, we performed a linear discriminant analysis (LDA) on the aligned coordinates with species as a classifier using MASS package version 7.3-53. PCA and LDA were performed using the entire dataset including both species, both sexes, and both fore- and hindwings to define wing traits in a common shape space. We also performed a principal components analysis (PCA) on the covariance matrix of natural logarithmic values of the five size traits (total body length, thorax width, abdomen length, wing length, and width of the S4 segment) for both species and sexes. We log-transformed the values for the size traits before running the PCA, so that the resultant PC values are mean-standardized. We averaged values obtained from left and right side of the wing of an individual whenever both sides were measured. When only one side of the wing was available, we used that available side as a representative measure. Since we found no directional asymmetry in wing shape in two species we examined (results not shown), this will unlikely create systematic bias in our measurements. In 62 individuals, we obtained scan images twice at two independent scanning sessions to evaluate measurement error due to variation in our imaging process and found that the measurement errors in aligned coordinates associated with the

difference in images are on average 0.19% of the centroid size (range: 0% - 3.34%, Fig. S2). Since this level of error is negligeable compared to the effect sizes of all analyses presented in this research, it will not be accounted for in subsequent statistical analyses of wing shape.

Quantifying social organization and mating system: For quantitative estimation of social organization in the two damselfly species, we measured the following parameters: male density (total number of males caught per sampling event / total catching time, unit = number of individuals captured per minute), female density (total number of males caught per sampling event / total catching time, unit = number of individuals captured per minute), operational sex ratio (ratio of the number of mature males to the number of mature females of a species caught at a locale in a given year, unit = %), androchrome frequency (ratio of the number of the androchrome female morph of a species to the total number of females of a species whose morph was identified in one locale in one year, unit = %), the proportion of copulating males (number of males in copula / total number of males caught during one sampling event, unit = %) and the opportunity for sexual selection (I_s, variance in male mating success / (average male mating success)^2, unitless elasticity) (Arnold & Wade, 1984). We estimated I_s for every locale from where we sampled populations of *E. cyathigerum* and *I. elegans*. Male mating success was defined as a binomial variable that could be either 0 or 1. We calculated variance in male mating success based on the data on the proportion of single and copulating males at each site and mean male mating success. The latter (mean male mating success) was calculated by the mean proportion of male (belonging to one species) mating at a particular locale in one field season (e.g., 0.10 if 10% are found in copula). The variance in mating success was evaluated as $\frac{p\times(1-p)}{n}$ where p is the probability of being found as a couple and n is the sample size.

Selection gradients: We used standard multiple-regression analyses to estimate the selection gradients (Lande & Arnold, 1983). Selection gradients were evaluated for body size (size-PC1) and wing shape (LD1) using mating success in the field as a male fitness component and the number of eggs laid as the female fitness component. Both linear (β) and quadratic (γ) selection coefficients were estimated for both species and sexes for all the traits using linear mixed effect models with locale as the random factor. The partial regression coefficients of models that includes only linear (i.e. unsquared) term were used to estimate β, while γ was estimated as the partial regression coefficients of models that includes both unsquared and squared terms. The quadratic regression coefficients and associated standard errors were multiplied by two (Stinchcombe *et al.*, 2008). Note that these operations are not necessary for quadratic terms between different traits (i.e. correlational selection). The quadratic selection surfaces were visualized using cubic splines (Schluter, 1948). Fitness components (mating success for male and the number of eggs laid for females) were standardized within species and sexes, by dividing individual fitness with the mean fitness estimates (De Lisle & Svensson, 2017). We chose to relativize fitness at the species level because the goal of this analysis is to characterize and compare selection between two species. This is equivalent to view populations of *I. elegans* and *E. cyathigerum* as two panmictic populations, which is justified if these populations represent different part of one global and shared fitness surface. Since both size-PC1 and wing shape LD1 are scaled to its own value either by taking a natural logarithm of size measurements or by performing the Generalized Procrustes Analyses, selection gradients evaluated in these traits are on the mean-standardized scale without

additional transformations. For comparison, we also estimated the variance-standardized selection gradients by dividing them with standard deviation of the trait within species. We also performed bivariate model to evaluate correlational selection between LD1 and size-PC1. We analyzed forewings and hindwings separately in these analyses because LD1 of fore- and hindwings are highly correlated (results not shown).

Estimation of selection gradients and statistical comparisons of adaptive landscape between species were made using random mixed effect models implemented in lme4 package (Bates *et al.*, 2015). We constructed three sets of models, which all included sampling location as the random effect. First, for each sex and species separately, we modeled fitness component as the response variable and one of examined traits (size-PC1, forewing shape LD1, hindwing shape LD1) and its squared terms as the fixed explanatory variables. Second, we constructed two bivariate models, for each sex and species separately, with the same model specifications as above but include either size-PC1 and forewing shape LD1 or size-PC1 and hindwing shape LD1 and their interaction and squared terms as the fixed explanatory variables. Finally, we constructed two models for each sex separately, with the fitness component as the response variable, size-PC1 and forewing shape LD1 or size-PC1 and hindwing shape LD1 with their squared terms, species (either *I. elegans* or *E. cyathigerum*) and interaction terms between species and all traits as the fixed explanatory variables. In the last model, we identified the best model with a backward model selection procedure based on AICc (sample size-corrected Akaike Information Criterion) values. In this approach, a comparison of AICc between two nested models with and without a focal parameter provides statistical support for the effect of the focal parameter.

Selection gradients and social organization: We evaluated the relationship between directional/quadratic selection gradients and local sexual selection regime across populations using a linear regression. For this analysis, we retained 14 populations with unique year-locale identity in *I. elegans* and 3 populations in *E. cyathigerum* that are represented by 20 or more samples and estimated linear (β) and quadratic (γ) selection gradients at each population as described above, but without locale as a random effect. In this analysis, we standardized fitness within populations and sexes by dividing individual fitness with the mean fitness estimated at corresponding populations. Our rationale is again to relativize fitness at the same level as the level at which comparisons of selection gradients are made. Another reason in favor of population-level standardizing is that the selection we estimate is considered soft (sensu De Lisle and Svensson 2017), that is, we hypothesize that the magnitude of selection is defined in the context of a population where selection operates. Using estimates of β and γ from these analyses, we constructed models where trait- and sex-specific selection gradients are the response variable and one of the six variables that describe social organization (male density, female density, operational sex ratio, androchrome frequency, mating frequency, opportunity for selection) are the predictor variable and species as the fixed effect that allows species to have different intercepts. Interaction terms between predictor variables were assessed but are not presented because none were statistically significant (results not shown). In all models, inverse of standard errors of selection gradients were used to weight observations to account for uncertainties in selection gradients. All analyses were performed in R version 4.2.2 and visualization of data and results were performed using ggplot2 package version 4.0.5.

Results

Dimension reduction of body size and exploration of wing morphospace: A scatterplot of the first two principal components of five body size measurements (Fig. S3) revealed that the first PC axis explained the vast majority (93.0%) of the total variation in log of body size measurements. Based on this, we hereafter use this axis (size-PC1) as our measure of body size. A scatterplot of the first two principal components of the entire wing shape data (including both species, sex, and both fore- and hindwings) is shown in Figure S4. The first principal component (shape-PC1) explained 41.9% of the total variation, and this axis separates forewings from hindwings in terms of the width of the wing. The forewings of both species have lower PC1 values along PC1 axis, which can be interpreted to narrower wings, while the hindwings of both species have higher values of PC, translating to broader wings. The second principal component (shape-PC2) explained 19.2% of the total variation in wing shape, and this axis separates the two species. *E. cyathigerum* has broader proximal edge and narrower distal edge of wings as compared to *I. elegans*. Subsequent PC axes up to PC5 explained 8.9%, 6.3%, and 5.9% of total variation, respectively.

A linear discriminant function analysis (LDA) with species as a grouping factor revealed that the axis that most effectively separates wings of the two species (wing shape LD1) explains 33.3% of the total variation in wing shape and represents the variation in the width of the wing, that occurs together with the stretch of two landmarks (LM9 and LM16) at the center of wing (Fig. 2). LD1 is correlated with shape-PC1 (r^2; forewing: 62.5%, hindwing: 68.6%) and shape-PC2 (r^2; forewing: 86.9%, hindwing: 89.0%), but not with shape PC3, PC4, and PC5 ($r^2 < 5\%$, Fig. S5). Within two subsets of data that include either forewings or hindwings, LD1 explained 47.1% (forewing) and 57.4% (hindwing) of the phenotypic variation within each of the subset, meaning that LD1 is the primary axis of phenotypic variation in these traits. In addition, LD1 captures variation that are most relevant for the goal of our study to compare adaptive landscape between *I. elegans* and *E. cyathigerum*. Moreover, given that our working hypothesis is that the two species reside at different parts of a shared adaptive landscape, studying LD1 will make our results conservative because we examine *similarity* of the adaptive landscape in the most *divergent* axis of wing morphospace. For these reasons, the rest of our analyses will use LD1 as a representative wing shape trait.

Selection gradients: Selection gradients evaluated at the species level are presented in Table 1. Across both species, we found that selection favors females with large body sizes. Estimates of mean-standardized directional selection gradients (β) in females (*I. elegans*: $\beta \pm SE = 1.569 \pm 0.295$, *E. cyathigerum*: 4.138 ± 0.545) means that doubling of body size would increase relative fitness by 157% in *I. elegans* and 414% in *E. cyathigerum*. In males, selection on size PC1 was weaker, whereas the quadratic selection gradients (γ) in *E. cyathigerum* indicate disruptive selection ($\gamma \pm SE = 5.551 \pm 2.726$) in favor of either small or large individuals.

Selection on wing shape LD1 was relatively weak across both sexes in both species (Fig. 3, Table 1). Estimates of β showed that the selection typically favors narrow and elongated wings in *I. elegans* while broad and round wings are favored in *E. cyathigerum*. Considering the mean shape differences between the two species (Fig. 2), these estimates suggest that, if all else being equal, directional selection would drive the convergent evolution of wing shape. The quadratic selection gradients (γ) suggested stabilizing selection (i.e., negative γ) on wing shape LD1 in all trait-sex-species combination except for forewing of *E. cyathigerum,* although none of these negative

410 estimates were significantly different from zero (Table 1). Therefore, wing shape appear to be
411 under weak stabilizing selection in both *I. elegans* and *E. cyathigerum*, and the result of β that
412 favors intermediate wing shape of the two species is consistent with the hypothesis that the two
413 species are evolving on different sides of a shared adaptive peak. For both size PC1 and wing
414 shape LD1, variance-standardized gradients showed qualitatively equivalent results (Table 1).
415 Results of correlational selections between wing shape and body size are presented in
416 Supplementary Material (Table S1, Fig. S6, S7).

417

418 **Comparison of adaptive landscape between species**: Comparisons of the adaptive landscape
419 between *I. elegans* and *E. cyathigerum* are summarized in Table 2. Pair-wise comparisons between
420 a model and its nested model based on AICc values indicate that the adaptive landscape is
421 divergent between the two species in terms of the quadratic terms of body size in males (*Δ*AICc =
422 6.6 in a model with forewing, *Δ*AICc = 7.3 in a model with hindwing) and in terms of the linear
423 term of body size in females (*Δ*AICc = 7.8 in a model with forewing, *Δ*AICc = 8.3 in a model with
424 hindwing). Thus, the disruptive selection on male body size in *E. cyathigerum* is absent or even
425 takes the form of stabilizing selection in *I. elegans* (Table1, Fig. 3A) while in females, directional
426 selection favoring large body sizes is stronger in *E. cyathigerum* than in *I. elegans* (Table1, Fig.
427 3D).

428

429 **Selection gradients at population levels and sexual selection regime**: Selection gradients
430 evaluated at 17 populations with unique species-locale-year identity are presented in Table S2-S5.
431 By comparing linear (β) and quadratic (γ) selection gradients at these population between *I.*
432 *elegans* and *E. cyathigerum*, we found no statistical evidence that the local fitness surfaces are
433 different between the two species (Fig. 4, Table S6). β on body size was far more variable than β
434 on wing shape (variance of β: male body size = 2.36, female body size = 10.1, male forewing
435 shape LD1 = 0.062, female forewing shape LD1 = 0.19, male hindwing shape LD1 = 0.021, female
436 hindwing shape LD1 = 0.027, unit: (relative fitness/$\log_e$(mm))^2 for body size, (relative
437 fitness/centroid size)^2 for wing shape), which globally fits with selection estimates at the species
438 level that the adaptive landscape of wing shape was similar between the two species whereas that
439 of body size showed more variation. Because γ was poorly estimated in most populations due to
440 small sample sizes (Table S2-S6), rest of analyses will be performed on β.

441 The summary of models relating β with social organization indices estimated at corresponding
442 location and year are shown in Figure 5, Table S7 and Table S8. We found that the strength of
443 directional selection on male body size is correlated with operational sex ratio (slope ± SE = 0.61
444 ± 0.15, $p < 0.01$) and opportunity for sexual selection (slope ± SE = 12.43 ± 4.95, $p = 0.025$), and
445 that a non-significant trend exists with respect to androchrome frequency (slope ± SE = -4,43 ±
446 2.57, $p = 0.11$). These relationships (Fig. 5) suggest that large male body sizes are favored in
447 populations where operational sex ratio is male-based, opportunity for sexual selection is high, and
448 androchrome females (male-mimicking morph) are rare. Visual inspection of these relationships
449 in *I. elegans* and *E. cyathigerum* as well as the lack of statistical support for the interaction term
450 between species and one of social organization indices in all examined models (Table S7, S8)
451 suggest that the local sexual selection regime influences the strength of directional selection in
452 male body size in a similar way in these two species. In addition, β on wing shape was related to
453 local sexual selection regime in terms of OSR and androchrome frequency (Table S8 and Figure

S8). Although these relationships were somewhat weaker than those on β on body size, the way by which social organization indices was related to the strength of selection was remarkably consistent between *I. elegans* and *E. cyathigerum*, suggesting that the adaptive landscape of body size in these two species are governed by similar ecological processes.

Discussion

Research on phenotypic selection in natural populations has been a popular and largely successful endeavor (Endler, 1986; Mitchell-Olds & Shaw, 1987; Wade & Kalisz, 1990; Kingsolver & Diamond, 2011), but its relevance to macroevolutionary dynamics remains poorly understood. In this study, we investigated if fluctuating selection in contemporary populations could still result in a stable adaptive zone over macroevolutionary time scale. By estimating linear and quadratic selection on two fitness-related traits (body size and wing shape), we demonstrated that *I. elegans* and *E. cyathigerum* have a largely shared underlying adaptive landscapes with respect to wing shape, while the adaptive landscapes of body size were more divergent between the two species. In addition, by analyzing variation in selection at population level, we further showed that local variation in sexual selection on male body size seem to arise from differences in mating system indices such as the frequency of female colour morphs and operational sex ratios that differ among populations. Interestingly, local socioecological indices influenced selection in a qualitatively similar fashion across both species. Below, we link these findings on contemporary phenotypic selection with macroevolutionary theory.

Stability of a shared adaptive zone

One question that we aimed to address here is whether the adaptive landscape remains stable over long evolutionary time periods as has often been assumed in macroevolutionary models of phenotypic evolution (Simpson, 1944; Hansen, 1997; Estes & Arnold, 2007; Uyeda *et al.*, 2011). Estimates of linear and quadratic selection on wing shape in *I. elegans* and *E. cyathigerum* revealed that wing shape generally seems to experience weak stabilizing selection (Fig. 3, Table 1). There was no evidence of divergent selection on wing shape between these two species, suggesting that the general form in their adaptive landscapes of wing shape is relatively stable. This is quite remarkable, considering that these two species belong to genera that diverged about 12 million years ago (Swaegers *et al.*, 2014; Callahan & McPeek, 2016; Blow *et al.*, 2021). One interpretation of this finding is that wing shape is currently maintained around two species-specific adaptive peaks that are similar in form. Alternatively, these two species may occupy a shared adaptive zone with a single adaptive optimum. Our results are in favor of the latter scenario. Selection estimated at the species level revealed that, among eight estimates of directional selection gradients (β) that we evaluated, β on wing shape in *E. cyathigerum* were all positive in sign, whereas all β on wing shape in *I. elegans* were all negative in sign (Table 1). Based on the difference in wing shape between *E. cyathigerum* and *I. elegans* (Fig. 2), these estimates can be interpreted as convergent selection favoring an intermediate wing shape of these two species.

By plotting the population-specific selection gradients of wing shape together with the global selective surfaces of *E. cyathigerum* and *I. elegans* (Fig. 6), we found that selection often favors a

wing shape intermediate in between these two species, with a possible exception in hindwing of females where β seems to push populations to species' specific adaptive peaks (Fig. 6D). However, the apparent peak of *E. cyathigerum* reflects one population with small sample size (Höje A6, Table S4) and the strength of selection is the weakest in hindwing among the three traits examined. Therefore, our results are largely consistent with the idea that wing shape of *E. cyathigerum* and *I. elegans* are evolving under a shared adaptive zone. It is conceivable that the intermediate wing phenotype represents a global adaptive optimum determined by some fundamental mechanical and physiological demands of flight, that would constitute the primary optimum (Hansen, 1997). Each one of these two species may occupy a fraction of this adaptive zone according to their ecological mode of life (Simpson, 1944) that are similar but also exhibit subtle differences (Fig. S9, Supplementary Results). Our analyses illustrate that the adaptive zone can take stabilizing form of selection even when individual selection estimates at any given place and time may give an impression of directional selection (Table S2-S5). Our finding corroborates a scenario previously suggested in other study systems (Svensson & Sinervo, 2004; Haller & Hendry, 2014) and provides empirical evidence for why naïve interpretation of local selection estimates as representative of global fitness surface may be misleading (Mitchell-Olds & Shaw, 1987; Morrissey & Hadfield, 2012).

Compared to selection on wing shape, selection on body size was considerably more variable. Females in both species experienced positive directional selection towards large body size although this fecundity selection was stronger in magnitude in *E. cyathigerum* than in *I. elegans* (Fig. 3, Table 1, Table 2). Thus, the fitness benefits in terms of fecundity increased faster with female body size in *E. cyathigerum* than in *I. elegans*. Stronger sexual conflict and more intense male mating harassment in females of *I. elegans* compared to *E. cyathigerum* can potentially explain divergence in selection on female body size. Male mating harassment in *I. elegans* has been shown to be mainly directed towards high-fecundity females (Gosden & Svensson, 2009). In other insects such as *Drosophila*, large females have intrinsically higher fecundity but they also suffer more from male mating attempts that reduce these intrinsic fitness advantages of large females (Long *et al.*, 2009; Chenoweth *et al.*, 2015). In contrast to the situation in *I. elegans*, in *E. cyathigerum,* female fecundity benefits of large size might be less affected by male mating harassment because male mating harassment appear to be lower in this *E. cyathigerum* compared to *I. elegans* based on several mating system indices (Supplementary Results, Table S9, Fig. S9). A lower proportion of androchrome females in *E. cyathigerum* than in *I. elegans* is also worth noting here, as androchrome females in damselflies benefit from reduced male mating harassment as shown in many previous studies in the genus *Ischnura* (Robertson, 1985; Cordero *et al.*, 1998; Gosden & Svensson, 2009; Willink *et al.*, 2019; Blow *et al.*, 2021). The lower frequency of androchrome females in *E. cyathigerum* compared to *I. elegans* might therefore reflect relaxed mating harassment and reduced sexual conflict in the former species. In addition, female *E. cyathigerum* are more locally segregated from conspecific males of the same species, as previously documented in other species of this genus (Stoks, 2001; Steele *et al.*, 2011), whereas in *I. elegans*, males and females typically co-occupy the same microhabitat and sex ratios are more even in this species (Fig. S9). Sexual habitat segregation might therefore further release females of *E. cyathigerum* from the cost of male mating harassment, enabling them to enjoy greater fecundity advantages of large body size compared to *I. elegans*.

In males, we found divergent patterns of selection on body size between the two species (Fig. 3A).

Specifically, *I. elegans* is characterized by a weak (non-significant) stabilizing selection while *E. cyathigerum* experienced disruptive selection (Fig. 3A). These results indicate that sexual selection on male body size is highly context-dependent in these damselflies (see Supplementary Material for related results and discussions on correlational selection). Previous studies have shown that the form and magnitude of sexual selection in damselflies can vary in a fine spatial and temporal scale depending on local social structure, such as the density of female color morphs (Gosden & Svensson, 2008) or phenotypic distribution of male and female body sizes (Steele *et al.*, 2011).

Ecological causes of variation in selection

Fluctuating selection has been put forward as an explanation of slow macroevolutionary rates or stasis (Merilä *et al.*, 2001; Estes & Arnold, 2007; Uyeda *et al.*, 2011), but empirical studies of phenotypic selection have rarely attempted to connect this to the stability of adaptive zone. We evaluated selection across multiple populations from two species of damselflies and demonstrated considerable variation in selection. However, we found no consistent difference in selection evaluated at the local population level between *I. elegans* and *E. cyathigerum* (Fig. 4). This result corroborates the similarity in these two species' adaptive landscapes of wing shape at the species level. These data further suggest that the adaptive zone of wing shape has been stable and is largely shared between these two species, and might have been so for millions of years. However, it somewhat contradicts our finding that selection on body size evaluated at the species level seems to be different between the two species. Below, we propose that ecology can reconcile this discrepancy.

By investigating local sexual selection regimes on male body size, we found that selection on male body size became stronger when the operational sex ratio (OSR) was male-biased (Fig. 5A), when androchrome females were rare (Fig. 5B) and when the opportunity for selection (Arnold & Wade, 1984) was high (Fig. 5C). In insects that engage scrambling male-male competition, OSR and the opportunity for selection are important descriptors of mating systems, and have previously shown to be correlated with sexual selection regimes in water striders (Arnqvist, 1992) and ambush bugs (Punzalan *et al.*, 2010). Our findings of a trend that low androchrome frequency strengthen directional selection on male body size mirrors the result of Gosden and Svensson (2008) who demonstrated a similar pattern in *I. elegans* based on more extensive spatiotemporal replicates (60 populations over 5 years) than the present study (17 populations over 2 years). One explanation for this is that in populations where androchrome females are common, males might also suffer from male mating attempts due to mistaken mate recognition, as previously shown in *I. ramburii* (Gering, 2017). Consequently, in populations with high frequencies of androchrome females, smaller males might be favored to reduce similarity with androchrome females and thereby male-male interference.

We also found that the local social environments affected the strength of sexual selection in *I. elegans* and *E. cyathigerum* in a similar fashion, both in terms of body size (Fig. 5) and wing shape (Fig. S8). These results suggest that the adaptive landscapes in males of these two species are shaped by similar social factors. This similarity of selective regimes in the two species likely

585 reflects the shared ecological resemblance among different species of pond damselflies (McPeek
586 & Brown, 2000; Siepielski *et al.*, 2010). Thus, we propose that difference in the adaptive
587 landscapes of male body size evaluated at the species level (Fig. 3, Table 3) reflect differences in
588 social organization between *I. elegans* and *E. cyathigerum* (Supplementary Results, Table S9, Fig.
589 S9). A common mechanism that may largely drive sexual selection in both these species is the
590 negative frequency-dependent selection (NFDS) driven by the frequency of female-limited color
591 polymorphisms (Svensson *et al.*, 2005; Takahashi *et al.*, 2010; Le Rouzic *et al.*, 2015). As
592 discussed above, *I. elegans* and *E. cyathigerum* are exposed to slightly different kinds of sexual
593 selection due to their difference in the frequency of androchrome females. Thus, their sexual
594 selection dynamics are expected to oscillate around different equilibria, and these equilibria are
595 likely to be influenced by NFDS on the female color polymorphisms in both species. Although the
596 causal link between the pattern of selection and sexual selection regimes needs to be
597 experimentally verified, we tentatively suggest that the adaptive landscape between *I. elegans* and
598 *E. cyathigerum* are largely shared because of shared ecological features, social organization and
599 mating systems.

600

601 **Conclusions**

602

603 Our comparative selection study of two phenotypically and ecologically similar damselfly species
604 have revealed that the adaptive landscapes of two key traits: body size and wing shape are largely
605 similar in spite of the two species separated from each other >12 million years ago. We further
606 demonstrated that local mating system indices influenced selection of two species in a similar
607 fashion. We conclude that phenotypic selection measured in contemporary populations can
608 potentially explain macroevolutionary dynamics, at least when closely related species have largely
609 overlapped ecological niches. While the two-species approach presented here is limited in its scope
610 (but see Price 1997 for arguments in favor of two-species comparative studies), we hope that the
611 approach we used here will stimulate future empirical research on the relationship between
612 "adaptive landscape" and "adaptive zone" as a bridge between micro- and macroevolution (Arnold
613 *et al.*, 2001). Phenotypic selection studies replicated across multiple species that covers wide range
614 of phenotype space and ecological circumstances is clearly the way forward for a more
615 comprehensive understanding of the links between of micro- and macroevolution.

References

Arnold, S.J., Pfrender, M.E. & Jones, A.G. 2001. The adaptive landscape as a conceptual bridge between micro- and macroevolution. *Genetica* **112–113**: 9–32.

Arnold, S.J. & Wade, M.J. 1984. On the measurement of natural and sexual selection: theory. *Evolution (N Y)* **38**: 709–719.

Arnqvist, G. 1992. Spatial variation in selective regimes: sexual selection in the water strider, Gerris odontogaster. *Evolution (N Y)* **46**: 914–929.

Bates, D., Maechler, M., Bolker, B.M. & Walker, S. 2015. Fitting linear mixed-effects models using lme4. Journal of Statistical Software 67: 1–48.

Blow, R., Willink, B. & Svensson, E.I. 2021. A molecular phylogeny of forktail damselflies (genus Ischnura) reveals a dynamic macroevolutionary history of female colour polymorphisms. *Mol Phylogenet Evol* **160**: 107134. Elsevier.

Brodie, E.D., Moore, A.J. & Janzen, F.J. 1995. Visualizing and quantifying natural selection. *Trends Ecol Evol* **10**: 313–318.

Callahan, M.S. & McPeek, M.A. 2016. Multi-locus phylogeny and divergence time estimates of Enallagma damselflies (Odonata: Coenagrionidae). *Mol Phylogenet Evol* **94**: 182–195. Elsevier Inc.

Chenoweth, S.F., Appleton, N.C., Allen, S.L. & Rundle, H.D. 2015. Genomic Evidence that Sexual Selection Impedes Adaptation to a Novel Environment. *Current Biology* **25**: 1860–1866. Elsevier Ltd.

Chevin, L. & Lande, R. 2015. Evolution of environmental cues for phenotypic plasticity. *Evolution (N Y)* **69**: 2767–2775. Wiley Online Library.

Corbet, P.S. 1999. *Dragonflies: behaviour and ecology of Odonata.* Harley books.

Cordero, A., Carbone, S.S. & Utzeri, C. 1998. Mating opportunities and mating costs are reduced in androchrome female damselflies, Ischnura elegans (Odonata). *Anim Behav* **55**: 185–197. Elsevier.

De Lisle, S.P. & Svensson, E.I. 2017. On the standardization of fitness and traits in comparative studies of phenotypic selection. *Evolution (N Y)* **71**: 2313–2326.

De Villemereuil, P., Charmantier, A., Arlt, D., Bize, P., Brekke, P., Brouwer, L., *et al.* 2020. Fluctuating optimum and temporally variable selection on breeding date in birds and mammals. *Proceedings of the National Academy of Sciences* **117**: 31969–31978. National Acad Sciences.

Endler, J.A. 1986. *Natural selection in the wild*. Princeton University Press.

Estes, S. & Arnold, S.J. 2007. Resolving the paradox of stasis: models with stabilizing selection explain evolutionary divergence on all timescales. *Am Nat* **169**: 227–244. The University of Chicago Press.

Gering, E.J. 2017. Male-mimicking females increase male-male interactions, and decrease male survival and condition in a female-polymorphic damselfly. *Evolution (N Y)* **71**: 1390–1396. Blackwell Publishing Inc Malden, USA.

Gosden, T.P. & Svensson, E.I. 2009. Density-dependent male mating harassment, female resistance, and male mimicry. *Am Nat* **173**: 709–721. The University of Chicago Press.

Gosden, T.P. & Svensson, E.I. 2008. Spatial and temporal dynamics in a sexual selection mosaic. *Evolution (N Y)* **62**: 845–856.

Grant, P.R. & Grant, B.R. 2002. Unpredictable evolution in a 30-year study of Darwin's finches. *Science (1979)* **296**: 707–711. American Association for the Advancement of Science.

Haller, B.C. & Hendry, A.P. 2014. Solving the paradox of stasis: squashed stabilizing selection and the limits of detection. *Evolution (N Y)* **68**: 483–500. Blackwell Publishing Inc Malden, USA.

Hansen, T.F. 1997. Stabilizing selection and the comparative analysis of adaptation. *Evolution (N Y)* **51**: 1341–1351. Wiley Online Library.

Hansen, T.F. 2014. Use and misuse of comparative methods in the study of adaptation. In: *Modern phylogenetic comparative methods and their application in evolutionary biology*, pp. 351–379. Springer.

Hansen, T.F., Pienaar, J. & Orzack, S.H. 2008. A comparative method for studying adaptation to a randomly evolving environment. *Evolution (N Y)* **62**: 1965–1977. Blackwell Publishing Inc Malden, USA.

Hereford, J., Hansen, T.F. & Houle, D. 2004. Comparing strengths of directional selection: how strong is strong? *Evolution (N Y)* **58**: 2133–2143. Wiley Online Library.

Kingsolver, J.G. & Diamond, S.E. 2011. Phenotypic selection in natural populations: what limits directional selection? *Am Nat* **177**: 346–357. University of Chicago Press Chicago, IL.

Kingsolver, J.G., Hoekstra, H.E., Hoekstra, J.M., Berrigan, D., Vignieri, S.N., Hill, C.E., *et al.* 2001. The strength of phenotypic selection in natural populations. *Am Nat* **157**: 245–261. The University of Chicago Press.

Kinnison, M.T. & Hendry, A.P. 2001. The pace of modern life II: from rates of contemporary microevolution to pattern and process. *Genetica* **112**: 145–164. Springer.

Lande, R. 1976. Natural selection and random genetic drift in phenotypic evolution. *Evolution (N Y)* 314–334. JSTOR.

Lande, R. & Arnold, S.J. 1983. The Measurement of Selection on Correlated Characters. *Evolution (N Y)* **37**: 1210.

Le Rouzic, A., Hansen, T.F., Gosden, T.P. & Svensson, E.I. 2015. Evolutionary time-series analysis reveals the signature of frequency-dependent selection on a female mating polymorphism. *American Naturalist* **185**: E182–E196.

Long, T.A.F., Pischedda, A., Stewart, A.D. & Rice, W.R. 2009. A cost of sexual attractiveness to high-fitness females. *PLoS Biol* **7**.

MacColl, A.D.C. 2011. The ecological causes of evolution. *Trends Ecol Evol* **26**: 514–522. Elsevier.

McPeek, M.A. & Brown, J.M. 2000. Building a regional species pool: diversification of the Enallagma damselflies in eastern North America. *Ecology* **81**: 904–920. Wiley Online Library.

Merilä, J., Sheldon, B.C. & Kruuk, L.E.B. 2001. Explaining stasis: microevolutionary studies in natural populations. *Genetica* **112**: 199–222. Springer.

Mitchell-Olds, T. & Shaw, R.G. 1987. Regression analysis of natural selection: statistical inference and biological interpretation. *Evolution (N Y)* **41**: 1149–1161. Wiley Online Library.

Morrissey, M.B. & Hadfield, J.D. 2012. Directional selection in temporally replicated studies is remarkably consistent. *Evolution* **66**: 435–442. Wiley Online Library.

Nishida, T. 1989. Is lifetime data always necessary for evaluating the "intensity" of selection? *Evolution (N Y)* **43**: 1826–1827. Blackwell Publishing Inc Malden, USA.

Nishida, T. 1994. Spatio-temporal variation of natural and sexual selection in breeding populations of the coreid bug, Colpula lativentris (Heteroptera: Coreidae). *Res Popul Ecol (Kyoto)* **36**: 209–218. Springer.

Opedal, Ø. 2021. A functional view reveals substantial predictability of pollinator-mediated selection. *J Pollinat Ecol* **30**: 273–288.

Phillips, P.C. & Arnold, S.J. 1989. Visualizing multivariate selection. *Evolution (N Y)* **43**: 1209–1222. Wiley Online Library.

Porto, A. & Voje, K.L. 2020. ML-morph: A fast, accurate and general approach for automated detection and landmarking of biological structures in images. *Methods Ecol Evol* **11**: 500–512.

Punzalan, D., Rodd, F.H. & Rowe, L. 2010. Temporally variable multivariate sexual selection on sexually dimorphic traits in a wild insect population. *Am Nat* **175**: 401–414. The University of Chicago Press.

Robertson, H.M. 1985. Female dimorphism and mating behaviour in a damselfly, Ischnura ramburi: females mimicking males. *Anim Behav* **33**: 805–809. Elsevier.

Schindelin, J., Arganda-Carreras, I., Frise, E., Kaynig, V., Longair, M., Pietzsch, T., *et al.* 2012. Fiji: An open-source platform for biological-image analysis. *Nat Methods* **9**: 676–682.

Schluter, D. 1996. Adaptive radiation along genetic lines of least resistance. *Evolution (N Y)* **50**: 1766–1774. Wiley Online Library.

Schluter, D. 1948. Evolution: An international journal of organic evolution. *Nature* **161**: 162–163.

Siepielski, A.M., Dibattista, J.D. & Carlson, S.M. 2009. It's about time: The temporal dynamics of phenotypic selection in the wild. *Ecol Lett* **12**: 1261–1276.

Siepielski, A.M., DiBattista, J.D., Evans, J.A. & Carlson, S.M. 2011. Differences in the temporal dynamics of phenotypic selection among fitness components in the wild. *Proceedings of the Royal Society B: Biological Sciences* **278**: 1572–1580.

Siepielski, A.M., Gotanda, K.M., Morrissey, M.B., Diamond, S.E., DiBattista, J.D. & Carlson, S.M. 2013. The spatial patterns of directional phenotypic selection. *Ecol Lett* **16**: 1382–1392. Wiley Online Library.

Siepielski, A.M., Hung, K.-L., Bein, E.E.B. & McPeek, M.A. 2010. Experimental evidence for neutral community dynamics governing an insect assemblage. *Ecology* **91**: 847–857. Wiley Online Library.

Siepielski, A.M., Morrissey, M.B., Buoro, M., Carlson, S.M., Caruso, C.M., Clegg, S.M., *et al.* 2017. Precipitation drives global variation in natural selection. *Science (1979)* **355**: 959–962. American Association for the Advancement of Science.

Simpson, G.G. 1944. *Tempo and Mode in Evolution*. Columbia University Press, New York.

Smallshire, D. & Swash, A. 2020. *Europe's Dragonflies - A field guide to the damselflies and dragonflies*.

Steele, D.B., Siepielski, A.M. & Mcpeek, M.A. 2011. Sexual selection and temporal phenotypic variation in a damselfly population. *J Evol Biol* **24**: 1517–1532.

Stinchcombe, J.R., Agrawal, A.F., Hohenlohe, P.A., Arnold, S.J. & Blows, M.W. 2008. Estimating nonlinear selection gradients using quadratic regression coefficients: Double or nothing? *Evolution (N Y)* **62**: 2435–2440.

Stoks, R. 2001. What causes male-biased sex ratios in mature damselfly populations? *Ecol Entomol* **26**: 188–197. Wiley Online Library.

Svensson, E. & Calsbeek, R. 2012. *The adaptive landscape in evolutionary biology*. OUP Oxford.

Svensson, E. & Sinervo, B. 2000. Experimental excursions on adaptive landscapes: density-dependent selection on egg size. *Evolution (N Y)* **54**: 1396–1403. Wiley Online Library.

Svensson, E.I. & Abbott, J. 2005. Evolutionary dynamics and population biology of a polymorphic insect. *J Evol Biol* **18**: 1503–1514.

Svensson, E.I., Abbott, J. & Härdling, R. 2005. Female polymorphism, frequency dependence, and rapid evolutionary dynamics in natural populations. *Am Nat* **165**: 567–576. The University of Chicago Press.

Svensson, E.I., Arnold, S.J., Bürger, R., Csilléry, K., Draghi, J., Henshaw, J.M., *et al.* 2021. Correlational selection in the age of genomics. *Nat Ecol Evol* **5**: 562–573. Springer US.

Svensson, E.I. & Sinervo, B. 2004. Spatial scale and temporal component of selection in side-blotched lizards. *Am Nat* **163**: 726–734. The University of Chicago Press.

Svensson, E.I., Willink, B., Duryea, M.C. & Lancaster, L.T. 2020. Temperature drives pre-reproductive selection and shapes the biogeography of a female polymorphism. *Ecol Lett* **23**: 149–159.

Swaegers, J., Janssens, S.B., Ferreira, S., Watts, P.C., Mergeay, J., McPeek, M.A., *et al.* 2014. Ecological and evolutionary drivers of range size in C oenagrion damselflies. *J Evol Biol* **27**: 2386–2395. Wiley Online Library.

Takahashi, Y., Kagawa, K., Svensson, E.I. & Kawata, M. 2014. Evolution of increased phenotypic diversity enhances population performance by reducing sexual harassment in damselflies. *Nat Commun* **5**: 1–7. Nature Publishing Group.

Takahashi, Y., Yoshimura, J., Morita, S. & Watanabe, M. 2010. Negative frequency-dependent selection in female color polymorphism of a damselfly. *Evolution (N Y)* **64**: 3620–3628. Blackwell Publishing Inc Malden, USA.

Uyeda, J.C., Hansen, T.F., Arnold, S.J. & Pienaar, J. 2011. The million-year wait for macroevolutionary bursts. *Proceedings of the National Academy of Sciences* **108**: 15908–15913. National Acad Sciences.

Wade, M.J. & Kalisz, S. 1990. The causes of natural selection. *Evolution (N Y)* **44**: 1947–1955.

765 Walsh, B. & Blows, M.W. 2009. Abundant genetic variation+ strong selection= multivariate genetic
766 constraints: a geometric view of adaptation. *Annu Rev Ecol Evol Syst* **40**: 41.
767 Willink, B., Duryea, M.C. & Svensson, E.I. 2019. Macroevolutionary origin and adaptive function of a
768 polymorphic female signal involved in sexual conflict. *Am Nat* **194**: 707–724. The University of
769 Chicago Press Chicago, IL.
770 Willink, B., Duryea, M.C., Wheat, C. & Svensson, E.I. 2020. Changes in gene expression during female
771 reproductive development in a color polymorphic insect. *Evolution (N Y)* **74**: 1063–1081.
772 Wright, S. 1932. The roles of mutation, inbreeding, crossbreeding, and selection in evolution.
773

Main Figures:

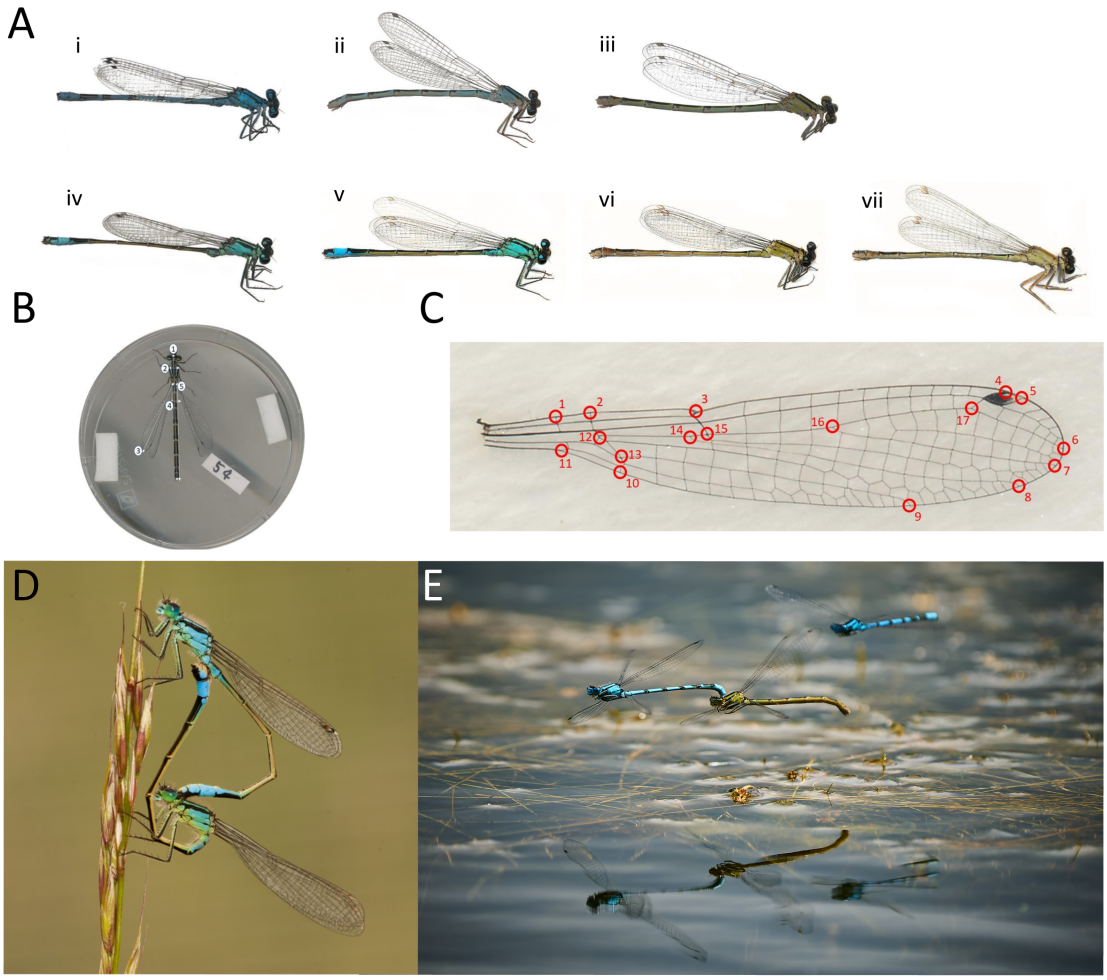

Figure 1: A) Males and female phenotypes and different color morphs in *E. cyathigerum* (i to iii) and *I. elegans* (iv to vii). Each subpanel shows an image of the following phenotype: males (i, iv), androchrome female (ii, v), gynochrome female (iii), infuscans female (vi), *infuscans-obsoleta* female (vii). Note that in both *E. cyathigerum* and *I. elegans* there is a male-mimicking female morph (androchrome females) but in former species there is only one gynochrome color morph, whereas in the latter there are two (*infuscans* and *infuscans-obsoleta*, respectively). B) Morphometric measurements of a female *E. cyathigerum* (all other males and females of *E. cyathigerum* and *I. elegans* were also measured similarly); 1: body length, 2: thorax width, 3: wing length, 4: width of abdomen segment S4, and 5: total abdomen length; C) 17 landmark position on a left forewing of a male *E. cyathigerum* that were used for estimation of the wing shape (all other males and females of *E. cyathigerum* and *I. elegans* were also landmarked similarly). D) a mating pair of *I. elegans* forming a mating wheel. E) a pair of *E. cyathigerum* forming a tandem.

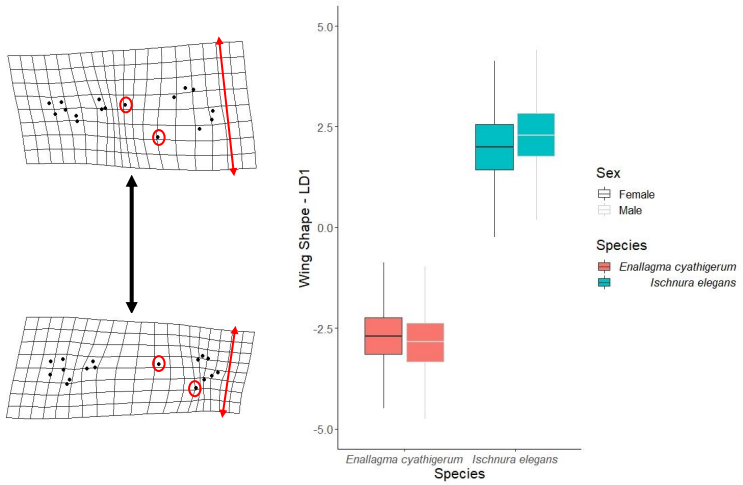

Figure 2: Boxplot comparing wing shape (LD1) between *I. elegans* and *E. cyathigerum.* The landmark specimens visualized in this figure represent shape associated with 2 times the minimum and maximum values of LD1.

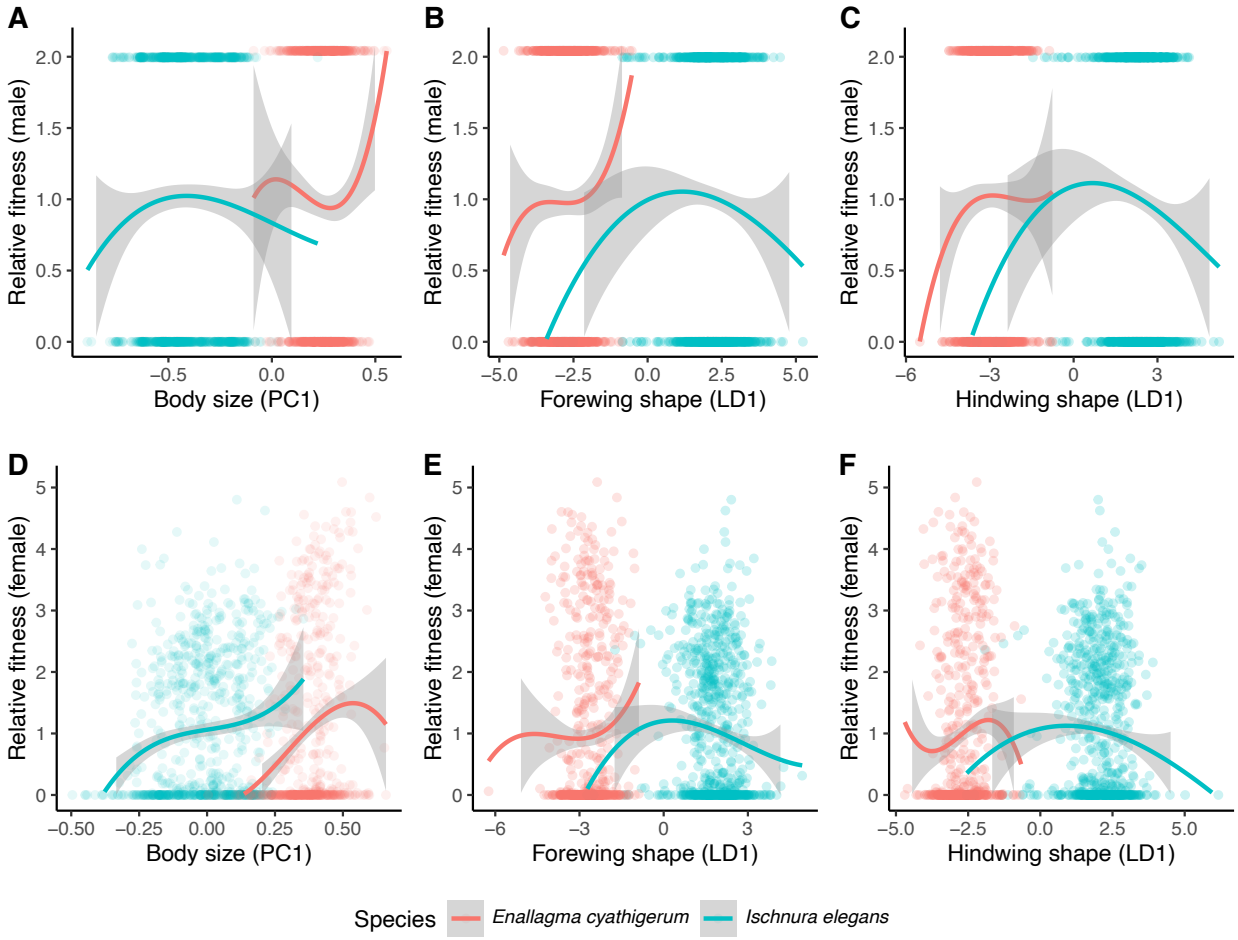

Figure 3: Univariate sexual selection (males, A-C) and fecundity selection (females, D-F) on body size (PC1) and wing shape (LD1) in *E. cyathigerum* and *I. elegans.* Fitness functions were visualized using cubic splines. Fitness data on the Y-axis were relativized at each species. The gray shaded regions around each spline represents the 95% confidence intervals. A) Selection on body size (PC1) in males, B) Selection on male forewing shape (LD1), C) Selection on male hindwing shape (LD1), D) Selection on body size (PC1) in females, E) Selection on female forewing shape (LD1) F) Selection on female forewing wing shape (LD1). The estimates for the coefficients of selection are presented in Table 1.

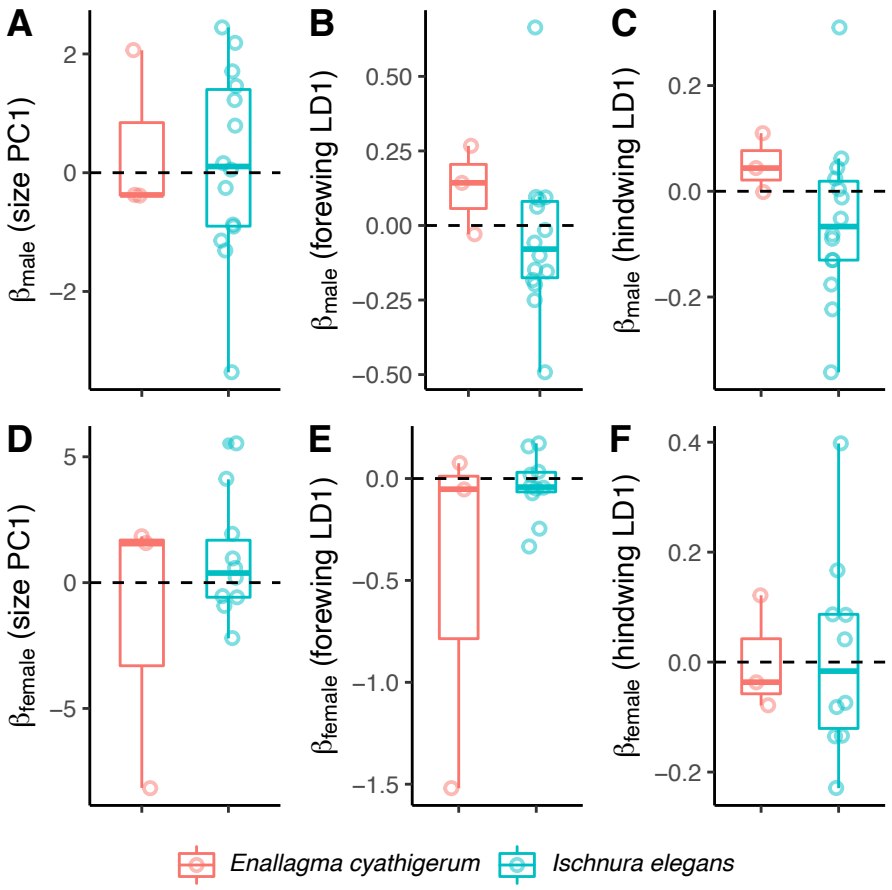

Figure 4. Boxplots (barline in the boxplot represent 50th percentile and the intervals represent the range between 1.5 times above 75th percentile and below 25th percentile) comparing linear selection gradients (β) between *E. cyathigerum* and *I. elegans* evaluated at 17 populations. β of A) male body size, B) male forewing shape, C) male hindwing shape, D) female body size, E) female forewing shape, F) female hindwing shape are compared. The estimates for the mean and standard errors of these parameters are as well as the statistical analysis for comparison between the two species (none are statistically different between the species) is presented in Table S6.

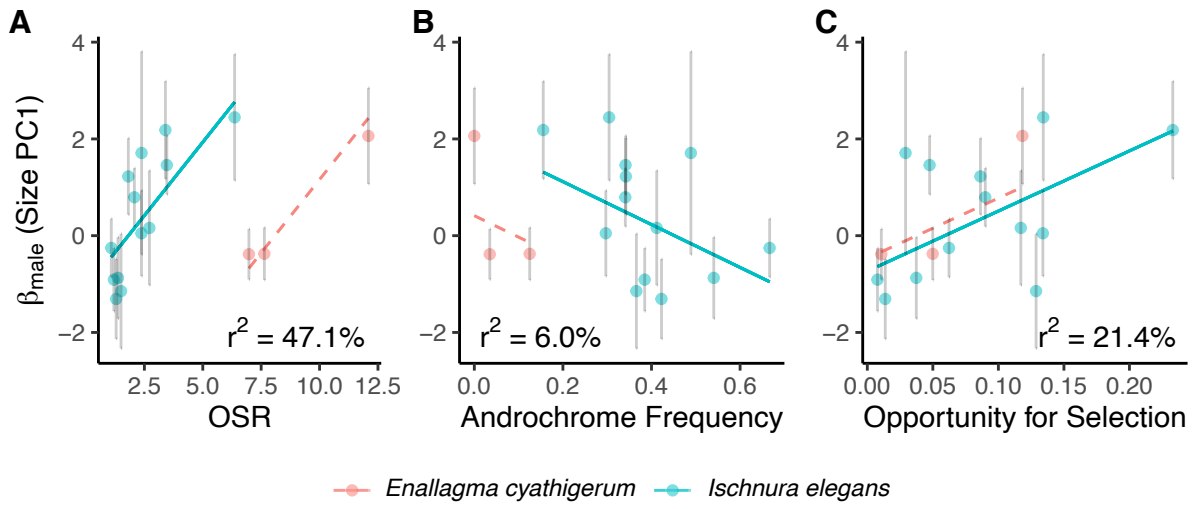

Figure 5: Relationship between directional selection gradient on male body size and (A) operational sex ratio (OSR), (B) androchrome frequency, (C) opportunity for selection. Each point represents a population with unique species-locale-year identity and error bar shows standard errors of selection gradients. Regression lines are derived from a weighted regression model (shown in Table S2-S5). Note that one population (*I. elegans* from Hoje A7 in 2021, see Table S2 for estimates of this population) was removed from plots for better visualization, while the regressions are from analyses using the whole dataset.

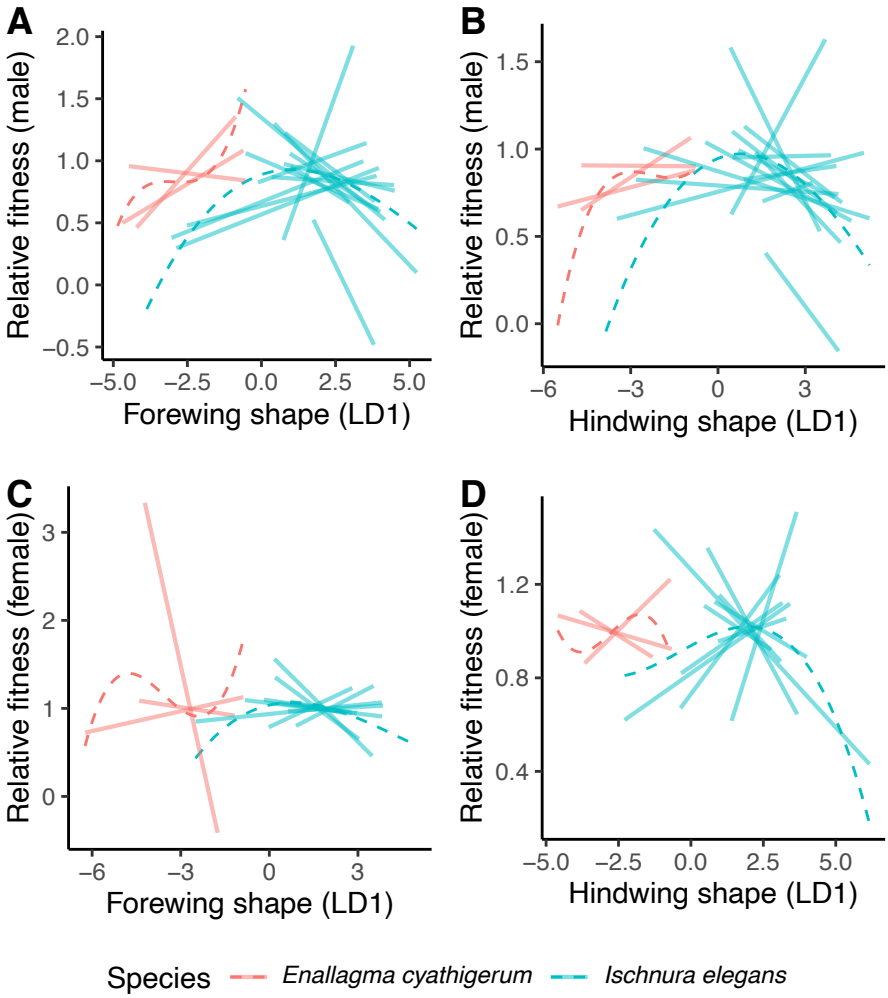

Figure 6. Comparison of species-specific fitness surface with directional selection gradients at each locality (3 populations in *E. cyathigerum* and 14 populations in *I. elegans*). Sexual selection (males, A-B) and fecundity selection (females, C-D) on wing shape (LD1, both fore- and hindwings) are plotted. Fitness functions of each species (dashed lines) were visualized using cubic splines. Fitness data on the Y-axis were relativized at each location. Directional selection gradients (solid lines) were estimated using a regression model of relative fitness against LD1 at each location. Estimates of these models are presented in Table S2-S5. A) Selection on male forewing shape (LD1), B) Selection on male hindwing shape (LD1), C) Selection on female forewing shape (LD1) D) Selection on female forewing wing shape (LD1).

Table 1: Mean-standardized univariate linear (β) and quadratic (γ) selection gradients for body size (PC1), and wing shape (LD1) to complement Figure 4. Estimates within square brackets "[]" are variance-standardized selection gradients. Estimates that are statistically significantly different from 0 at a significance level of $p < 0.05$ are shown in **bold**. All estimates are obtained from mixed-effect models that include sampled location as a random effect.

Trait	**Sex**	**β ± SE**		**γ ± SE**	
		I. elegans	*E. cyathigerum*	*I. elegans*	*E. cyathigerum*
Body size PC1	♂	0.053±0.200	-0.036±0.388	-3.234±2.026	**5.551±2.726**$^{(*)}$
		[0.008±0.032]	[-0.003±0.036]	[-0.082±0.052]	[**0.094±0.046**$^{(*)}$]
	♀	**1.569±0.295**$^{(***)}$	**4.138±0.545**$^{(***)}$	-3.761±3.275	-5.578±6.698
		[**0.222±0.042**$^{(***)}$]	[**0.415±0.055**$^{(***)}$]	[-0.076±0.066]	[-0.056±0.067]
Wing shape LD1 (forewing)	♂	-0.018±0.036	0.080±0.057	**-0.057±0.027**$^{(*)}$	0.133±0.109
		[-0.015±0.032]	[0.050±0.036]	[**-0.064±0.025**$^{(*)}$]	[0.049±0.046]
	♀	**-0.112±0.050**$^{(*)}$	0.137±0.091	**-0.090±0.041**$^{(*)}$	0.145±0.145
		[**-0.094±0.042**$^{(*)}$]	[0.086±0.057]	[-0.074±0.039]	[0.054±0.064]
Wing shape LD1 (hindwing)	♂	-0.051±0.036	0.046±0.054	**-0.052±0.025**$^{(*)}$	-0.145±0.087
		[-0.045±0.032]	[0.030±0.036]	[**-0.065±0.024**$^{(**)}$]	[-0.056±0.047]
	♀	-0.063±0.050	**0.194±0.094**$^{(*)}$	-0.071±0.036	-0.137±0.186
		[-0.052±0.042]	[**0.118±0.057**$^{(*)}$]	[-0.064±0.036]	[-0.059±0.074]

Note: * indicates $0.01 < p < 0.05$, ** indicates $0.001 < P < 0.01$, *** indicates $p < 0.001$.

Table 2. Model selection evaluating the difference of selection gradients between species. A full list of variables in a model and associated AICc values are presented. Note that the location of capture was included as a random effect in all models considered. The best model (i.e. a model with the lowest AICc) within a nested models are shown in **bold**.

Sex	Model	AICc
♂	MS~FWLD1+FWLD1^2+PC1+PC1^2+Species+Species:FWLD1+Species:FWLD1^2+Species:PC1+Species:PC1^2	5139.1
	MS~FWLD1+FWLD1^2+PC1+PC1^2+Species+Species:FWLD1+Species:FWLD1^2+Species:PC1^2	5140.5
	MS~FWLD1+FWLD1^2+PC1+PC1^2+Species+Species:FWLD1^2+Species:PC1^2	5139.7
	MS~FWLD1+FWLD1^2+PC1+PC1^2+Species+Species:PC1^2	**5133.2**
	MS~FWLD1+FWLD1^2+PC1+PC1^2+Species	5139.8
	MS~HWLD1+HWLD1^2+PC1+PC1^2+Species+Species:HWLD1+Species:HWLD1^2+Species:PC1+Species:PC1^2	5163.6
	MS~HWLD1+HWLD1^2+PC1+PC1^2+Species+Species:HWLD1+Species:HWLD1^2+Species:PC1^2	5165.1
	MS~HWLD1+HWLD1^2+PC1+PC1^2+Species+Species:HWLD1+Species:PC1^2	5159.9
	MS~HWLD1+HWLD1^2+PC1+PC1^2+Species+Species:PC1^2	**5156.5**
	MS~HWLD1+HWLD1^2+PC1+PC1^2+Species	5163.8
♀	Fec~FWLD1+FWLD1^2+PC1+PC1^2+Species+Species:FWLD1+Species:FWLD1^2+Species:PC1+Species:PC1^2	4377.1
	Fec~FWLD1+FWLD1^2+PC1+PC1^2+Species+Species:FWLD1+Species:FWLD1^2+Species:PC1	4379.8
	Fec~FWLD1+FWLD1^2+PC1+PC1^2+Species+Species:FWLD1+Species:PC1	4377.2
	Fec~FWLD1+FWLD1^2+PC1+PC1^2+Species+Species:PC1	**4373.8**
	Fec~FWLD1+FWLD1^2+PC1+PC1^2+Species	4381.6
	Fec~HWLD1+HWLD1^2+PC1+PC1^2+Species+Species:HWLD1+Species:HWLD1^2+Species:PC1+Species:PC1^2	4384.5
	Fec~HWLD1+HWLD1^2+PC1+PC1^2+Species+Species:HWLD1+Species:HWLD1^2+Species:PC1	4387.2
	Fec~HWLD1+HWLD1^2+PC1+PC1^2+Species+Species:HWLD1+Species:PC1	4382.0
	Fec~HWLD1+HWLD1^2+PC1+PC1^2+Species+Species:PC1	**4378.5**
	Fec~HWLD1+HWLD1^2+PC1+PC1^2+Species	4386.8

Note: Abbreviations are used to indicate the following variables; MS: mating success, FW: forewing, PC1: size PC1, HW: hindwing, Fec: fecundity